ASSESSMENT OF THE UO_2 FUEL DOPING IMPACT ON CANDU FUEL PERFORMANCE

ELENA MATEI [1], ROXANA MIHAELA ROMAN [2], IOSIF PRODEA [1], IOANA NEACȘU [1] and DRAGOȘ VICTOR IONESCU [1]

[1] Institute for Nuclear Research (RATEN ICN) Pitești, Romania
[2] Technologies for Nuclear Energy State Owned Company, Romania
e-mail: elena.matei@nuclear.ro

Abstract

The aim of the paper is to analyze the accident tolerant fuel (ATF) element behaviour under CANDU type reactor irradiation specific conditions, by means of FEMAXI-6 fuel performance code. Thermo-mechanical calculations for UO_2 fuel doped with different contents of Cr_2O_3 and Al_2O_3 have been carried out, and then the results were compared to those supplied by the CANDU standard UO_2 fuel, in order to assess the dopant' impact on the fuel performance. It is well known that the additive content influences pellet grain diameter and density, resulting in larger grains and increased density of doped fuel. Therefore, the ATF concept is expected to perform better in terms of operational safety. In this respect, the obtained results shown that the doped UO_2 fuel has lower fuel temperatures, reduced internal pressure, and improved fission gas retention compared to the CANDU standard UO_2 fuel.

Keywords: *CANDU, Accident Tolerant Fuel, Cr_2O_3 and Al_2O_3 dopants, thermo-mechanical calculations, FEMAXI-6 code*

Introduction

After the devastating East Japan Earthquake and Tsunami and subsequent events at the Fukushima Daiichi power plant, a global interest in developing innovative fuels within the framework of Accident Tolerant Fuel (ATF) concept, mainly UO_2 doped type, has been confirmed [1]. The ATF concepts have a great potential to increase the safety of CANDU reactors under all operational conditions, as well as during potential accident situations.

The ATF concepts improve fission product retention due to an increased grain size compared to the conventional UO_2 fuel used in PHWR reactors. The most used dopants, Chromium oxide (Cr_2O_3) and Aluminum oxide (Al_2O_3), facilitate densification and grain growth during sintering, leading to an improved microstructure [2].

A recent experimental program on the obtaining of UO_2 sintered pellets with large-grain size has been started by a research group from the Nuclear Materials, Corrosion and Surface Analysis Department of RATEN ICN Pitesti. The purpose of this research activity is to manufacture doped fuel pellets with enhanced grain size, about five to eight times larger, compared to that of the standard UO_2 fuel [3].

The current study aims to assess the ATF behaviour under CANDU type reactor normal operation specific conditions using the FEMAXI-6 fuel performance code. The simulations were carried out for CANDU standard UO_2 and UO_2 doped fuels with different content of dopants as follows: 0.05 wt%, 0.1 wt%, and 0.16 wt% Cr_2O_3, and a unique concentration of 0.02 wt% Al_2O_3 in all specimens.

In order to perform the FEMAXI-6 simulations, the input data files were prepared considering the geometric and fabrication characteristics along with irradiation conditions. Regarding the results, the focus was on the evolution of the following fuel performance parameters: temperatures, internal pressure, gap conductance, fission gas amount released in the internal free volume, and outer pellet diameter variation during irradiation. The conclusions highlighted the additives' impact on the fuel performance.

Modeling aspects

The methodology used in the present study included fuel element description and material properties as well as an overview on FEMAXI-6 code capabilities, by presenting the main simulation aspects relevant for analysis. The proposed ATF concept was developed starting from the standard CANDU fuel element, which keep the same geometric characteristics but has different pellet grain size and density. Zircaloy-4 was the cladding material considered, and the filling gas inside the fuel element consisted of 80% He and 20% N [3].

The UO_2 doped fuel's grain size and density have been experimentally measured, these data being also considered in FEMAXI-6 simulations. Table 1 presents the obtained doped fuel configurations, and it can be easily notice that the fuel grain size grows as the Cr_2O_3 content increase. The standard UO_2 fuel has an initial grain size of 10 μm and a density of 10.6 g/cm^3. The corresponding content of Cr_2O_3 in the doped fuel pellets was increased gradually up to the dopant's solubility limit in UO_2, in applicable sintering conditions [4].

Other relevant fuel element characteristics used in the input data files were, as follows: fuel pellet diameter - 12.22 mm, fuel element stack length - 481.8 mm, cladding outer diameter - 13.096 mm, and clad thickness - 0.39 mm.

Table 1. Analyzed fuel configurations

Dopant content (%)			Density (g/cm^3)	Fuel average grain size (μm)
	Cr_2O_3	Al_2O_3		
Case 1	0.05	0.02	10.86	45
Case 2	0.1		10.83	55
Case 3	0.16		10.81	63

FEMAXI-6 fuel performance code

The integrated fuel analysis code FEMAXI-6 has been developed by the JAEA (Japan Atomic Energy Agency, formerly Japan Atomic Energy Research Institute) to assess the behavior of nuclear fuels in normal operation conditions. Subsequent improvements allow FEMAXI-6 to cover both normal operation and transient conditions such as load-following and rapid power increase. However, it does not cover accident conditions such as Reactivity Insertion Accident (RIA) or Loss of Coolant Accident (LOCA) [5].

The code consists of two coupled main modules - thermal analysis and mechanical analysis module, as shown in Fig. 1.

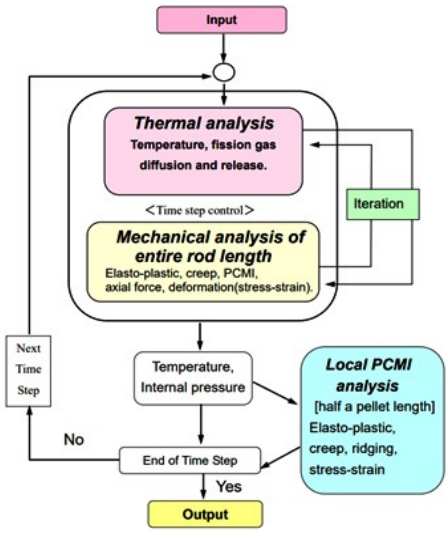


Fig. 1. Scheme of FEMAXI-6 code structure [5]

The two main modules cover the behaviour of the entire fuel rod. The thermal analysis module solves tasks related to the temperature distribution and fission gas release. The mechanical analysis part deals with the creep analysis, pellet cladding mechanical interaction, deformation etc. In each calculation time step, the convergence of temperature and deformation is required as a condition for approaching the next time step [5].

Material properties of the standard UO_2 and doped fuels

The material properties of the doped and standard UO_2 fuels are presented in the following as they are included in FEMAXI-6 code input data files and used in the current analysis. Taking into account that the doped UO_2fuel has similar properties to the standard UO_2 one, the same model correlations were used in simulation for both fuel types.

All the used correlations are typical models included in FEMAXI-6 code. Therefore, the MATPRO-Version 09 model for thermal conductivity, Young's modulus, Poisson's ratio, and thermal expansion coefficient were considered, along with the White model for fission gas atom diffusion constant equation, the FEMAXI III model for pellet densification, and the Itoh model (modified Ainscough) for the fuel grain growth [5, 6].

For the UO_2 fuel several correlations are included in FEMAXI-6 code, and MATPRO model was chosen for the present study.

UO_2 thermal conductivity

The main parameter with a strong influence on fuel temperature behaviour is the thermal conductivity. The thermal conductivity model is conducted by name-list input parameter IPTHCN, being given by the following formulas applicable to different temperature ranges:

$$K = \left[\frac{1-\beta(1-D)}{1-0.05\beta}\right]\cdot\left[\frac{40.4}{464+T}+1.216\cdot10^{-16}\cdot e^{1.867\cdot10^{-3}\cdot T}\right] \quad (1)$$

$$0 \le T \le 1650\ ^\circ C$$

$$K = \left[\frac{1-\beta(1-D)}{1-0.05\beta}\right]\cdot\left[0.0191+1.216\cdot10^{-16}\cdot e^{1.867\cdot10^{-3}\cdot T}\right] \quad (2)$$

$$1650\ ^\circ C < T \le 2840\ ^\circ C$$

where: K - thermal conductivity of UO_2 pellet (W/cm·K);
D - UO_2 theoretical density ratio;
T - temperature (°C); β - porosity coefficient;
$\beta = 2.58\text{-}0.58\cdot10^{-3}\cdot T$

UO_2 thermal expansion

Another important parameter for the proposed assessment is the pellet thermal expansion, managed by the input variable IPTHEX and calculated as follows:

$$\frac{\Delta L}{L} = -4.972\cdot10^{-4} + 7.107\cdot10^{-6}\cdot T + 2.581\cdot10^{-9}\cdot T^2 + 1.140\cdot10^{-13}\cdot T^3 \quad (3)$$

with: $\frac{\Delta L}{L}$ = linear thermal expansion; T = temperature (°C)

UO_2Young's modulus

The Young's modulus depends on temperature and theoretical density and it is given by the formula:

$$E = 2.26\cdot10^{11}(1-1.131\cdot10^{-4}\cdot T)[1-2.62(1-D)] \quad (4)$$

where: E - Young's modulus (Pa); T - temperature (°C);
D - theoretical density ratio.

For the *UO_2 Poisson's ratio,* υ, a constant value of 0.316 is used.

Fission gas atom diffusion constant equation

FEMAXI-6 code contains several options for the fission gas atom diffusion constant equation, selected by the input variable IDCNST. For the proposed analysis, in present paper the White model was used:

$$D = AM1 \cdot 7.6 \cdot 10^{-10} e^{\frac{-7 \cdot 10^4}{RT}} + 1.5 \cdot 10\sqrt{R} \cdot e^{\frac{-10600}{T}} + \\ + 7.67 \cdot 10^{-22} R \cdot e^{\frac{-2785}{T}} \quad (5)$$

where: T - temperature (K); R - universal gas constant(J·s/g).

UO_2 densification

The following correlation was chosen for the pellet densification, selected by input option IDENSF, which is also the standard recommended model for FEMAXI-6:

$$\frac{\Delta V}{V} = \frac{\Delta V^{\max}}{V}(1 - e^{-C \cdot Bu}) \quad (6)$$

where: $\Delta V/V$ - volume contraction due to densification;

$\Delta V^{\max}/V$ - maximum volume contraction due to densification;

Bu - burnup (MWd/tUO_2).

UO_2 grain growth

The option of the grain growth model can be selected using IGRAIN, in our case MATPRO-09 model was inputted:

$$D^4 - D_0^4 = 6.18 \cdot 10^{13} \cdot e^{\frac{-92400}{RT}} \cdot t \quad (7)$$

where: D - grain size at time t (μm);

D_0 - initial grain size (μm);

R- gas constant 1.987 (cal/mol·K);

T - temperature (K); t - time (h).

UO_2 theoretical was assumed to be constant and equal to 10.96 g/cm^3.

The gap thermal conductance model was chosen setting up the input option IGAPCN=5, according to the FEMAXI bonding gap model.

ATF performance results and discussions

The results obtained from FEMAXI-6 simulations will be presented in the following along with a comparison between the doped and the standard UO_2 fuels.

From reactor operating experience and reactor physics calculations, it is well known that the outer ring elements of CANDU fuel are the most stressed, being subject to the highest linear power level in the fuel bundle. Consequently, obtaining the linear power distribution on the outer ring elements with respect to the fuel burnup (the so-called *"irradiation histories"*) is a prerequisite condition for the fuel element performance evaluation. In this respect, the irradiation histories for all selected working configurations (presented in Table 1) have been generated using the 3D finite differences 2-group DIREN program [7, 8] along with the WIMS transport code [9, 10] and associated library [11]. These values have been further converted in a specific FEMAXI-6 format, as illustrated in Figs. 2 and 3.

Depicting the maximum values of linear powers with respect to the burnup led to linear power envelopes generation for all working configurations, as shown in Fig. 4.

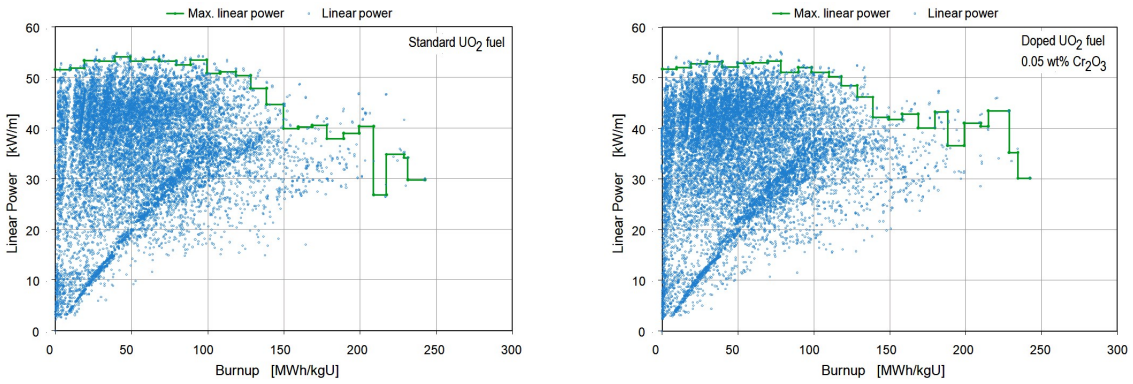


Fig. 2. Outer element linear power for standard UO_2 (left) and doped fuel 0.05 wt% Cr_2O_3 (right)

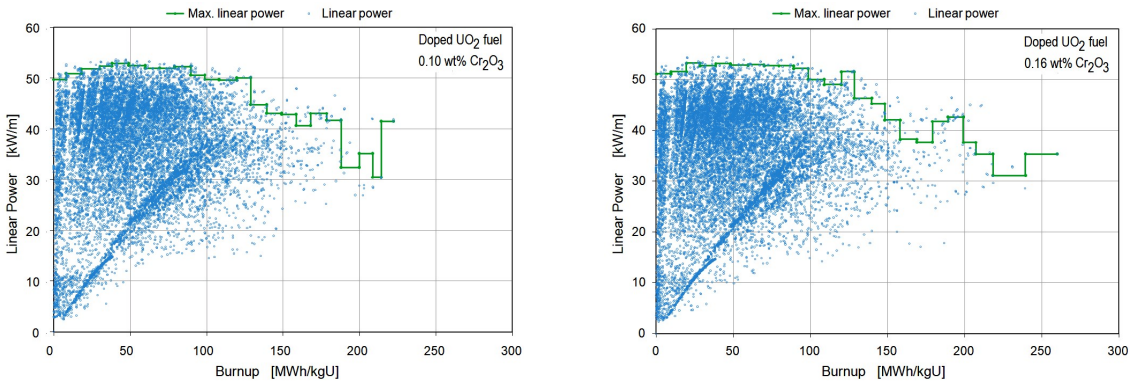


Fig. 3. Outer element linear power for doped fuel 0.1 w% Cr_2O_3 (left) and 0.16 wt% Cr_2O_3 (right)

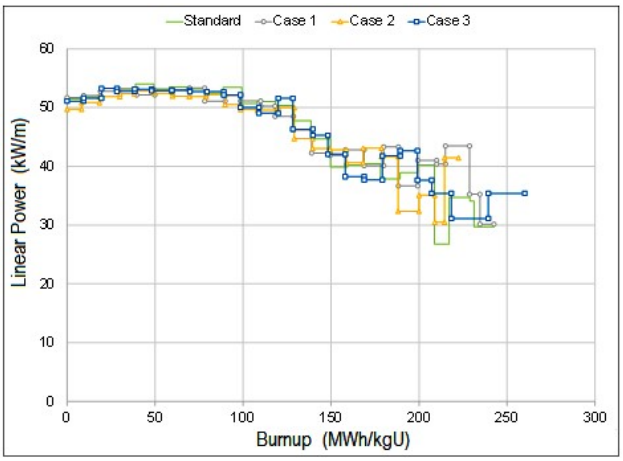


Fig. 4. Linear power envelopes for the considered cases

Based on the power envelopes shown in Fig. 4, FEMAXI-6 simulations have been carried out for the considered fuel configurations pursuing the following parameters: fuel temperatures, internal pressure, gap conductance, fission gas released in the internal free volume and outer pellet diameter.

The evolutions of fuel center temperature for standard and doped UO_2 fuels are comparatively presented in Fig. 5. For the ATF elements, the central temperature maximum values remain below 1700 °C, while for standard UO_2 fuel the temperature overrides 1800 °C, especially in the first part of the irradiation history.

Regarding the impact of Cr_2O_3 content in the UO_2 fuel, no significant differences were noticed between the studied cases (with Al_2O_3 content being constant). The ATF concept proves an improved behaviour in terms of fuel center temperature, which consequently may lead to an improved behaviour regarding the fission gas release.

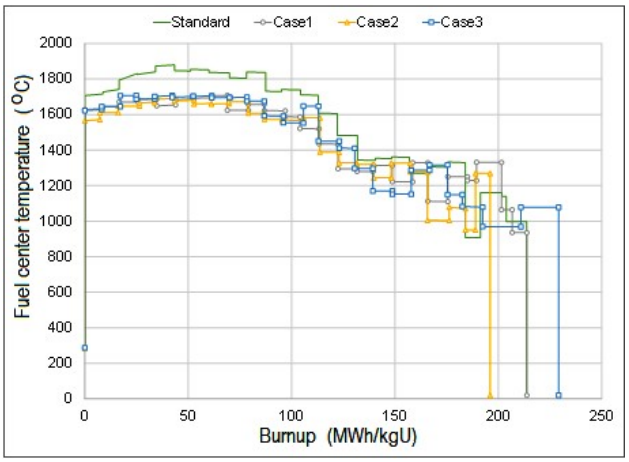


Fig. 5. Evolution of fuel center temperature for the considered cases

The fuel surface temperature evolution is represented in Fig.6, for the considered configurations. There were no significant changes in surface temperature values with respect to the dopant content. However, a difference of about 30 °C between the standard fuel and doped ones is revealed. This behavior proves again that the doped fuel configurations improve the nuclear safety.

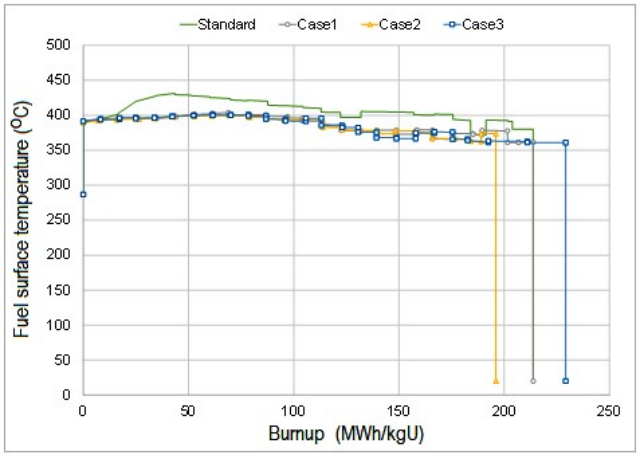


Fig. 6. Evolution of fuel surface temperature for the considered cases

According to the previous results, it is expected that a higher fuel temperature to lead to greater internal element pressures and fission gas release volumes. Figs. 7 and 8 illustrate the parameters alluded above.

As it can be noticed from Fig. 7, in case of the standard UO_2 fuel (Case Standard), the maximum internal pressure value reaches about 2.15 MPa, while the simulations for the doped fuels reveal significantly lower values, by about 50% in comparison to the standard fuel one. The maximum values do not exceed 1.25 MPa for the lowest Cr content configuration (0.05 wt% Cr_2O_3, Case 2), while an increased Cr content lead to the internal pressure decreasing (Case 2 and Case 3).

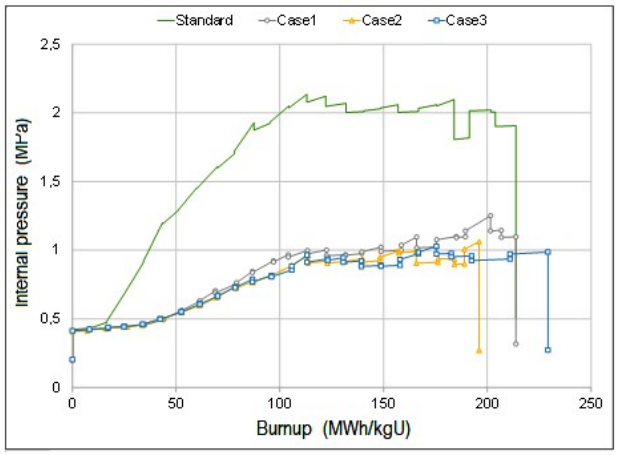


Fig. 7. Evolution of internal element pressure for the considered cases

The volume of fission gas release as function of burnup is illustrated in Fig. 8. The accumulation of fission gases in the fuel element free volume builds up the element internal pressure. It is worthy to mention that the lack of any dopant in the UO_2 fuel promotes free gasses released to significantly larger volumes, about twice larger than in the case of doped UO_2 fuel. During normal operation, the volume of fission gas release reaches 7.5 cm^3 for the standard UO_2 fuel case, while for the doped UO_2 fuel cases it doesn't exceed 4 cm^3, meaning about 50% reduction.

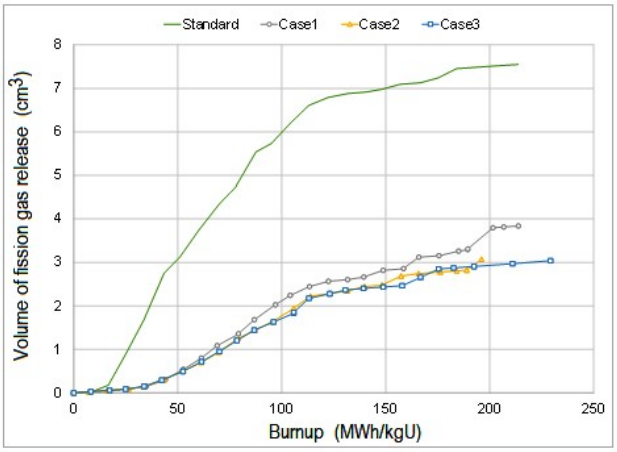


Fig. 8. Evolution of volume of fission gas release for the considered cases

Regarding the gap thermal conductance (HTC) parameter, its evolution is influenced by the gap dimension, as it can be seen in Fig. 9. Taking into account that the CANDU cladding is very thin and, by irradiation, it gradually collapses on the fuel stack, the largest gap size is revealed at the beginning of irradiation. When the gap dimension approaches to zero, the conductance reaches its maximum value, while when the gap opens more, HTC decreases. Higher HTC values were calculated for the standard UO_2 fuel, according to the fuel temperature evolution.

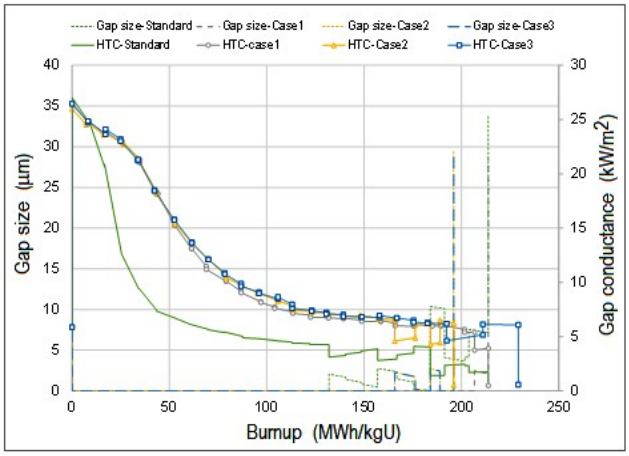


Fig. 9. Evolution of gap conductance and gap size for the considered cases

Another major aspect regarding the nuclear safety is the pellet-cladding mechanical interaction that can be assessed representing the outer pellet radius variation with respect to the fuel burnup. In the specific literature [12], it is recognized that the fuel pellet swelling phenomena can increase the cladding stresses. Fig. 10 reveals a similar behavior for the considered fuel configurations.

Nevertheless, the presence of dopants promotes the pellet radius to slightly higher values, especially at the end of fuel cycle. This behavior is in accordance to the better fission gases retention inside the doped fuel, and it cannot be a reason of worry due to the small differences revealed.

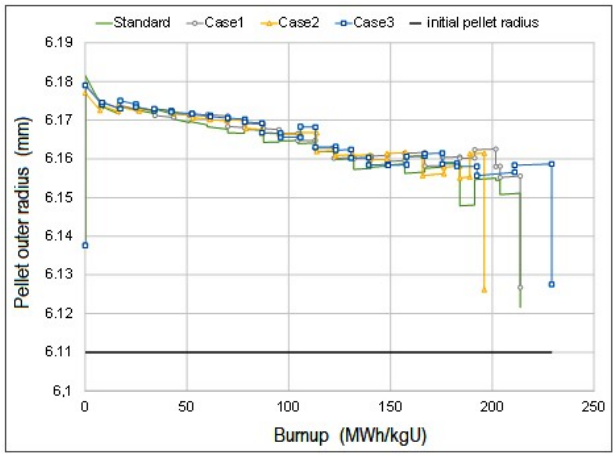


Fig. 10. Evolution of fuel pellet outer radius for the considered cases

Conclusions

The paper presents the results of fuel element performance calculations for large-grained Cr_2O_3 and Al_2O_3 doped CANDU UO_2 fuel. The simulations were carried out by using the FEMAXI-6 fuel performance code. The main assessed performance parameters were: fuel temperatures, internal pressure, fission gas release, gap conductance and pellet outer radius.

ATF doped elements emphasized a better thermal behaviour based on lower fuel center temperature by 100 ºC than the standard UO_2 fuel one, during most of the irradiation period. The same behaviour is shown by the fuel pellet surface temperature, where the using of Cr-Al dopants led to temperature reducing by about 7.5%, from 430 ºC to 400 ºC.

The most relevant improvements when using doped fuel are revealed by the element internal pressure and fission gas release, as lower value of these parameters is associated with an improved behaviour. The fission gas volume generated by the considered ATF configurations (4 cm^3) is only about a half of the gas volume associated to CANDU standard UO_2 fuel (7.5 cm^3), a major aspect for clad integrity maintaining. Internal gas pressure value of ATF configurations was also lower than the one corresponding to CANDU standard UO_2 fuel, the difference between being in the same ratio.

The gap size values for the ATF configurations assessed during the irradiation period were larger than the standard fuel one. As result, the fuel-clad interaction is less likely to occur in the case of ATF using.

Regarding the fuel pellet swelling phenomena, all the considered fuel configurations present similar decreasing of the fuel pellet radius by irradiation. As a result, the clad collapsing on the fuel pellet stack is not expected.

FEMAXI-6 simulations performed have proved that for the considered ATF configurations enhanced fuel performances in normal operation conditions were obtained.

Future work envisages assessment of ATF configurations based on using of metallic dopants like niobium and titanium, in both normal and transient conditions.

References

[1] Ohta, H. et al. (2016) ″Development of accident tolerant control rod for LWR″, Proc. of Top Fuel Int. Conf., paper 17556, American Nuclear Society, USA.

[2] Gamble, K.A., Pastore, G., Cooper, M.W.D. (2020) ″BISON Development and Validation for Priority LWR-ATF Concepts″, Technical Report INL/EXT-20-59969, rev.3, Idaho National Laboratory, USA, https://inldigitallibrary.inl.gov/sites/sti/sti/Sort_26886.pdf.

[3] Postelnicu, M. (2023) ″Studies on obtaining UO2 sintered pellets with large-grain size″, Internal Report R.I. 13377 (in Romanian), Institute for Nuclear Research, Pitesti, Romania.

[4] Riglet-Martial, Ch. (2014) ″Thermodynamics of chromium in UO_2 fuel: A solubility model″, *J. of Nuclear Materials*, Vol. 447(1-3), pp. 63-72.

[5] Suzuki, M., Saitou, H. (2005) "Light Water Reactor Fuel Analysis Code FEMAXI-6 (Ver.1) - Detailed Structure and User's Manual", JAEA-Data/Code, Japan.

[6] Hagrman, D.L., Reyman, G.A. (1979) ″MATPRO-Version11, A Handbook of Materials Properties for use in the analysis of light water reactor fuel rod behavior″, NUREG/CR-0497, TREE-1280, rev.3, Nuclear Regulatory Commission, USA.

[7] Pătrulescu, I. (2012) ″INR Coupled Reactor Physics and Thermal Hydraulics Calculation System for CANDU Reactor″, IAEA Workshop on Advanced Code Suites for Design, Safety Analysis and Operation of Heavy Water Reactors, Ottawa, Canada.

[8] Pătrulescu, I., Constantin, M., Radeș, E., Bălăceanu, V. (1997) ″Development of CANDU reactor physics calculation system based on WIMS code″, *Annals of Nuclear Energy*, Vol. 24 (14), pp. 1105-1125.

[9] Prodea, I., Văduva, M.R. (2024) ″Burnup Penalties for Some ATF Fuel Options in a CANDU Type Reactor″, *J. of Nuclear Research and Development*, No.28, pp.8-13.

[10] Nuclear Energy Agency (1991) ″WIMS-D4 -Winfrith Improved Multigroup Scheme Code System″, RSICC Computer Code Collection, CCC-576, ORNL-DOE, contributed by: Atomic Energy Establishment, Winfrith, Dorchester through the NEA Data Bank, France.

[11] International Atomic Energy Agency ″WLUP-WIMS Library Update Project″, http://www-nds.iaea.org/wimsd/libraries.htm, http://www-nds.iaea.org/wimsd/download/ iaea.zip

[12] OECD Nuclear Energy Agency (2019) ″Pellet-Clad interaction in Water Reactor Fuel″, OECD Publishing, https://www.oecd-nea.org/upload/docs/application/pdf/2019-12/6004-pellet-clad.pdf .